

Microstructure and properties of austenite-bainite steel matrix wear resistant composite reinforced by granular eutectics

XU ZHENMING*, LI TIANXIAO, LI JIANGUO

School of Materials Science and Engineering, Shanghai Jiao Tong University, Shanghai 200030, People's Republic of China

E-mail: zmxu@mail1.sjtu.edu.cn

A new austenite-bainite steel matrix wear resistant composite reinforced by granular eutectics (abbreviated ABGE composite) has been obtained by controlling the solidification structure of the steel melt, which only contains manganese and silicon, with modification of Al-Mg-Ce compound and air-hardening. It has been found that the granular eutectic is a pseudo-eutectic of austenite and $(\text{Fe,Mn})_3\text{C}$, which is formed between austenite dendrites during solidification due to the segregation of C and Mn enhanced by modifying elements. The granulation of the eutectic can be explained by the heterogeneous nuclei of MgS and CeO_2 and by the influence of the modifying elements on the crystallization of the eutectic. The eutectic and bainite contents are 4%–10% and 20%–40%, respectively. The size of the eutectic is $5\ \mu\text{m}$ – $20\ \mu\text{m}$ and its microhardness is HV800–1200. The wear resistance of the ABGE composite is much higher than that of the austenite-bainite steel, austenite-bainite ductile cast iron and medium manganese steel with nodular carbides under low and medium impact working condition because the granular eutectics effectively lighten the intrusion of abrasives into the worn surface and microcutting by abrasives on the worn surface and austenite-bainite matrix structure has high strain-hardening ability.

© 2001 Kluwer Academic Publishers

1. Introduction

Austenite-bainite steel as a wear-resistant material has been widely used because it has excellent properties [1–3]. However, the application of this steel is limited because it has poor wear resistance due to no particles phases in the matrix and austempering technology and large amount of molybdenum and nickel is needed to produce it. Wear resistant white cast iron has high wear resistance because the eutectic carbides can strongly resist abrasive wear but it has low strength and toughness. In order to ensure sufficient strength-toughness, it is necessary to design a new type of austenite-bainite steel matrix wear resistant composite reinforced by granular eutectics (abbreviated ABGE composite) which possesses the advantages of austenite-bainite steel and wear resistant white cast iron. In this research, the microstructure and properties of the ABGE composite has been studied.

2. Experimental

The chemical compositions of the steel are (wt%): 1.0–2.0C, 0.5–1.0Si, 3.0–5.0Mn. The steel was prepared by a non-oxidation process in a 5 Kg induction furnace. After de-oxidizing by aluminum, the steel

was poured at $1600\ ^\circ\text{C}$ and modified by Al-Mg-Ce compound 0.5–2.0 wt% added. Samples of dimensions $12\ \text{mm} \times 12\ \text{mm} \times 60\ \text{mm}$ were casted in sand moulds. The specimens were austenitized at $860\ ^\circ\text{C}$ for 40 min and hardened in air, then ground into $10\ \text{mm} \times 10\ \text{mm} \times 55\ \text{mm}$ size (without notch) for impact test, hardness test, wear test and observation of the metallographic structure. Transmission electron microscope (TEM) (H-800), scanning electron microscope (SEM) (JAX-840) and electron probe microanalyser (EPMA) were used in the observation and analysis. The content of bainite and eutectic in this composite is analyzed by VIDAS (Video and Image Digital Analysis System).

Wear tests were performed on a dynamically loaded abrasive wear testing machine, model ML-10 [4]. The test parameters were as follows: impact frequency, $100\ \text{rev}\ \text{min}^{-1}$; hammer weight, 10 kgf; impact energy, 0.5 J, 1.0 J, 1.5 J and 2.0 J; wearing time, 20 min. Abrasives of 3 mm–5 mm SiO_2 and CaCO_3 grain sizes were used in the test, so as to simulate the site working conditions of easily worn parts, such as hammers and the plate hammers of breaking machines and grinding balls of ball mills.

*Author to whom all correspondence should be addressed.

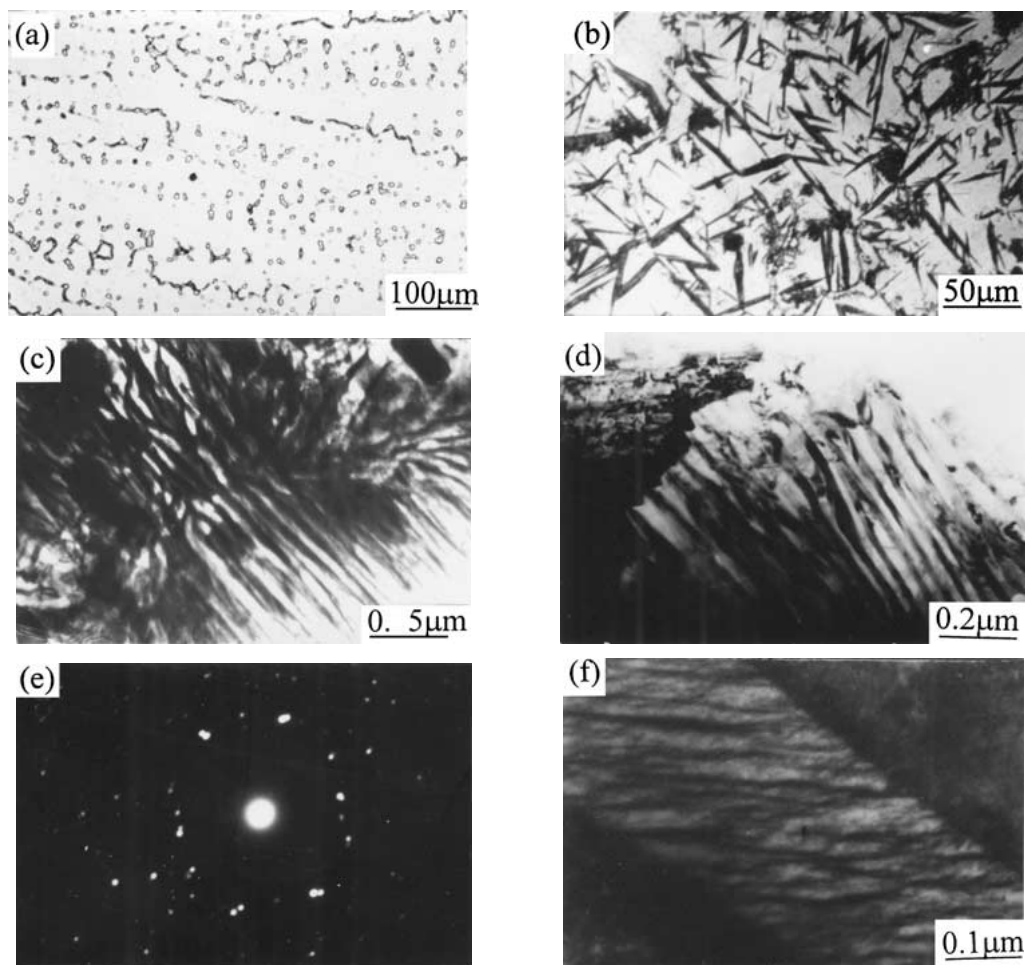


Figure 1 Metallographic structure of ABGE composite: (a) as-cast state (optical micrograph); (b) air-hardening (optical micrograph); (c) (d) morphology of the eutectic (TEM); (e) diffraction pattern of the eutectic, $B_{\gamma\text{-Fe}} = [011]$, $B_{(\text{Fe,Mn})_3\text{C}} = [234]$; (f) morphology of the bainite (TEM).

3. Results and discussion

3.1. Microstructure of ABGE composite

After the steel melt, which consists of only manganese and silicon, was modified by Al-Mg-Ce compound, numerous granular eutectic was dispersed in the austenite matrix, as shown in Fig. 1a. Fig. 1b shows the austenite-bainite matrix structure of the ABGE composite by air hardening. As shown in Fig. 1c and d, granular eutectic is a eutectic of austenite ($\gamma\text{-Fe}$) and cementite ($(\text{Fe,Mn})_3\text{C}$) by analysis of diffraction patterns (Fig. 1e). Its size is $5\ \mu\text{m}$ – $20\ \mu\text{m}$. Composition analysis by EPMA shows that the chemical composition of the eutectic is (wt%): 2.25C, 8.90Mn and 1.75Si.

Fig. 1f shows the bainite structure of the ABGE composite. It is different from the typical bainite. The residual austenite is distributed between ferrite plates and there is no carbide [5].

Fig. 2 shows the morphology and distribution of eutectic in the as-cast with the increment of modifying agent as follows: needle-like carbides [6] and granular eutectics \rightarrow large amount of granular eutectics \rightarrow granular eutectics and network eutectics at boundary of grains.

When the amount of modifying agent is 1.2%, the quantity of eutectic makes up 6.5% and it is dispersed inside the austenite grains. Fig. 3 shows the relation between adding amount of modifying agent and structure content of ABGE composite. It can be seen that the

formation of the eutectic is beneficial to the formation of the bainite because the C content in the austenite is decreased when numerous eutectics is formed, which makes B_s , the critical temperature at which the transition from austenite to bainite occurs during cooling, decrease. Thus, austenite easily transforms to bainite during cooling and the content of bainite increases.

3.2. Formation of the granular eutectic

Lattice constant of the austenite ($\gamma\text{-Fe}$) in the as-cast state (Fig. 1a) is defined by analysis of XRD (X-Ray Diffraction), then C content in $\gamma\text{-Fe}$ is calculated, as shown in Table I. It is seen that C content in $\gamma\text{-Fe}$ is decreased gradually with the increment of modifying agent because the modifying elements enhance segregation of C. Table II shows the effect of modification on segregation coefficients ($1 - K$) of Mn and Si. It is seen that the segregation coefficient ($1 - K$) of Mn increases from 0.136 to 0.265 with the increment of modifying

TABLE I Lattice constant and C content of austenite in cast steel

Quantity of modifying agent (wt%)	Lattice constant of $\gamma\text{-Fe}$ (nm)	C content of $\gamma\text{-Fe}$ (wt%)
0.00	0.3616	1.0170
0.40	0.3602	0.7068
0.80	0.3597	0.5980
1.20	0.3595	0.5430

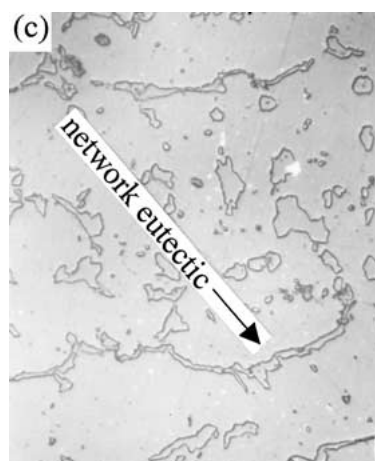
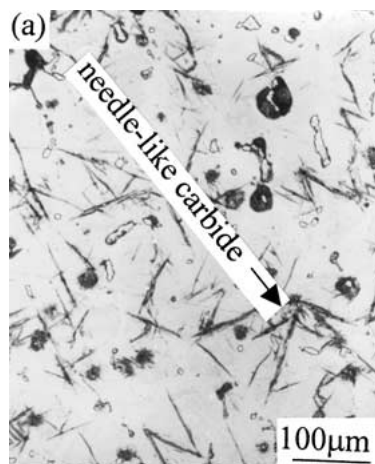


Figure 2 Effect of the adding amount of modifying agent on structure of the composite in the as-cast state: (a) 0.4 wt%; (b) 1.2 wt%; (c) 1.6 wt%.

agent, the increment ratio of the segregation coefficient of Mn has reached 95%. At the same time, Mn content in γ -Fe decreased gradually.

The microsegregation and distribution of alloying elements in the matrix, on the grain boundary, in the eutectic, or on the interface of the eutectic were analyzed using an electron probe. The analyzing results are given in Table III and Fig. 4a–c. It indicates that Ce, Mg and Al adsorb and enrich on the growing surface of the eutectic during crystallization. MgS and CeO₂ have been found in the eutectic in Fig. 4e and f and the eutectic grows on the basis of MgS and CeO₂. CeAlO₃ has also been found in the eutectic [7] under the same condition.

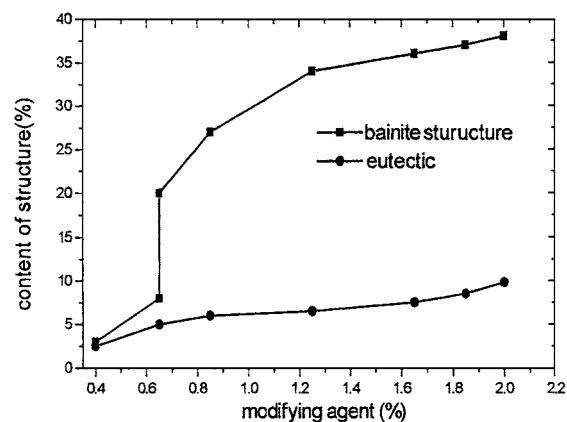


Figure 3 Effect of the adding amount of modifying agent on structure content of ABGE composite.

According to the mathematical model of two-dimensional lattice discrepancy [8], the lattice discrepancy between the (001) of Fe₃C and the (001) of MgS and between the (001) of γ -Fe and (001) of MgS are 8.10% and 2.35%, respectively. The lattice discrepancy between the (100) of Fe₃C and the (001) of CeO₂ and between the (001) of γ -Fe and (001) of CeO₂ are 9.39% and 7.13%, respectively. The values of the lattice discrepancy are all less than 12%. Therefore, MgS and CeO₂ can act as the heterogeneous nuclei for the eutectic crystallization.

During the solidification process, as the temperature decreases in the small molten regions located in the interstices between austenitic dendrite arms and austenitic grains, f_L (the volume fraction of the remaining liquid) becomes smaller and the contents of Al, Ce, Mg and O increase because their segregation coefficient values are less than 0.60, 0.02, 0.001 and 0.003, respectively [9]. When thermodynamic and dynamic conditions for the formation of MgS and CeO₂ is satisfied, MgS and CeO₂ forms preferentially in the small molten regions [10].

As solidifying, the contents of C and Mn in small remaining liquid regions between the austenite dendrites increase continuously because of the segregation of C and Mn enhanced by modifying elements. When the liquid in small molten regions meets the demand of the eutectic reaction at the end of the solidification, the eutectic is formed and the MgS and CeO₂ formed previously can act as heterogeneous nuclei for the eutectic phase, as shown in Fig. 4d and f.

When the eutectic grows, Ce, Mg, and Al elements have following functions: (1) In general, the eutectic cementite (Fe₃C) is leading phase during the eutectic growth because the crystallization model of the eutectic (austenite and eutectic cementite) is facet-nonfacet [11]. After the proper amount of Al-Mg-Ce compound being added, Ce and Mg elements adsorb on the surface of the preferred orientation [010] of the eutectic cementite, which makes the growing speed of the eutectic cementite in preferred orientation decreases. Therefore, the austenite and eutectic cementite grow at almost the same speed when the eutectic grows. (2) As solubility of Al is smaller in the cementite, Al element enriches on the growing interface of eutectic to impede

TABLE II Effect of modification on segregation coefficients ($1 - K$) of Mn and Si

Quantity of modifying agent, wt%	Cc in centre of dendrite, wt%		Cb at boundary of dendrite, wt%		$1 - K$ $K = Cc/Cb$
	Mn	Si	Mn	Si	
0.00	4.32	0.94	4.93	1.05	$1 - K_{Mn} = 0.136$
	4.35	1.09	4.97	1.24	$1 - K_{Si} = 0.142$
	4.16	0.93	4.95	1.16	
0.04	3.98	1.18	4.76	1.39	$1 - K_{Mn} = 0.158$
	4.13	1.23	4.95	1.47	$1 - K_{Si} = 0.135$
	3.89	1.29	4.55	1.42	
0.08	3.24	1.37	4.38	1.54	$1 - K_{Mn} = 0.251$
	3.53	1.51	4.59	1.75	$1 - K_{Si} = 0.128$
	3.15	1.48	4.27	1.71	
1.20	3.06	1.79	4.18	2.02	$1 - K_{Mn} = 0.265$
	2.98	1.87	4.26	2.13	$1 - K_{Si} = 0.124$
	3.15	1.86	4.07	2.15	

TABLE III Microdistribution of alloying elements (wt%)

Microarea	Composition							
	C	Mn	Si	Ce	Mg	Al	O	Fe
Matrix	0.58	4.12	1.74	0.00	0.00	0.00	0.00	Bal.
Eutectic	2.25	8.90	1.75	0.05	0.03	0.00	0.00	Bal.
Boundary of eutectic in matrix	0.67	5.23	1.07	0.02	0.05	0.15	0.00	Bal.
Interface of eutectic after eutectic removed	0.75	4.56	2.50	0.08	0.04	0.24	0.00	Bal.

Fe, C and Mn elements to pile on the eutectic when the eutectic grows. At the same time, the constitutional supercooling on the eutectic interface, which reduces the growing speed of the eutectic.

The above results indicate that the Ce, Mg and Al adsorb and enrich on growing surface of the eutectic during the crystallization, which makes the crystallization model of the eutectic turn from facet–non-facet to non-facet–non-facet. When the eutectic crystallizes as non-facet–non-facet, the growing speed of the eutectic is about the same in every orientation, the shape of the crystallization front of the eutectic is spherical surface and the inside structure of the eutectic is arranged as layers, as shown in Fig. 1c and d. Therefore, the granular eutectic is a pseudo-eutectic of austenite and Fe_3C (non-eutectic composition). The granulation of the eutectic can be explained by the heterogeneous nuclei of MgS and CeO_2 and by the influence of the modifying elements on the crystallization of the eutectic.

3.3. Mechanical properties and wear-resistance of ABGE composite

The microhardness of the eutectic is HV800-1200. The hardness and toughness of ABGE composite are listed in Figs 5 and 6. When the eutectic content (V_E) and bainite content (V_B) are 6.5% and 35% respectively, this composite has excellent match relationship of strengthening and toughening. It is because the needle-like carbides dispersed in austenite (as shown in Fig. 2a) are detrimental to toughness when the amount of the eutectic is less than 6.5%, and the network eutectics at boundary of grains (as shown in Fig. 2c) make the toughness decrease when the amount of the eutectic is more than 6.5%.

The grinding ball ($\Phi 80$ mm) was cast in sand mould, its hardness and toughness are 42-50HRC and more than $10 J cm^{-2}$ after air-hardening. It shows that this composite has good hardenability.

Figs 7 and 8 show that the eutectic and bainite contents on wear resistance of the ABGE composite under different impact energy. When V_E is equal to 6.5%, it has good wear resistance because the composite has good hardness and toughness. With the increment of the bainite content, the wear resistance increases gradually.

The wear test results are given in Table IV. Fig. 9 is the contrast diagram of wear resistance of ABGE composite ($V_E = 6.5\%$, $V_B = 35\%$) with existing wear-resistant materials. It can be seen that the wear resistance of the ABGE composite is higher than that of the austenite-bainite steel, austenite-bainite ductile cast iron and medium manganese steel with nodular carbides. Therefore, this composite is a promising candidate material to resist abrasive wear under low and medium impact working condition.

Fig. 10 is hardness distribution of the worn surface of ABGE composite under different impact energy. It can be seen that the worn surface hardness increases with the increment of impact energy. ABGE composite has high strain hardening ability.

Fig. 11a and b show that the worn surface morphologies for ABGE composite under 2.0 J and 0.5 J. It indicates that there are numerous plough channels formed by microcutting of abrasives and a few of peeling hole formed by fatigue peeling under low impact. There are numerous peeling hole formed by drilling and rolling fail and a few of plough channel formed by microcutting of abrasives under high impact. Therefore, the mechanism of wear loss effectiveness of this composite are:

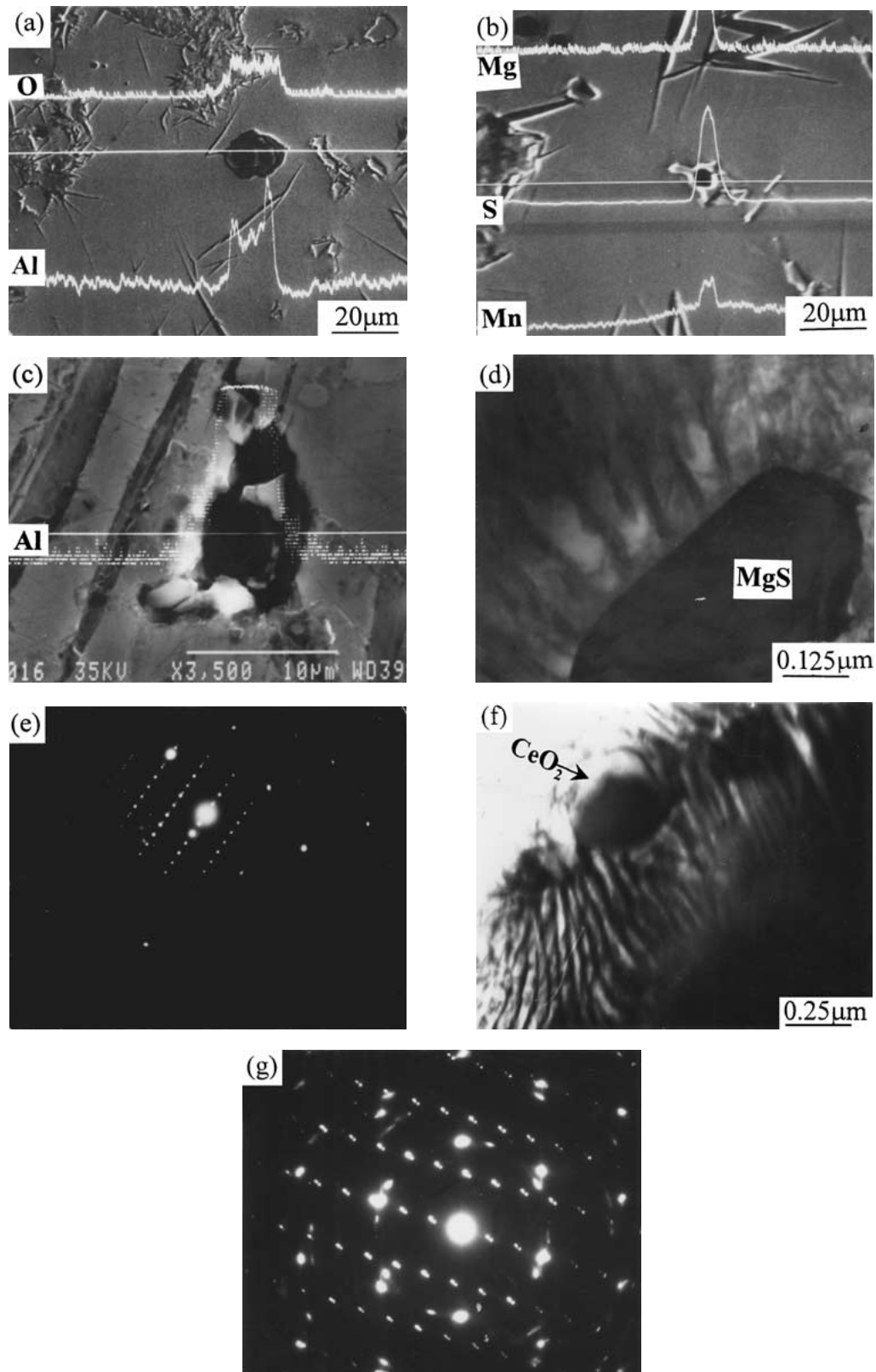


Figure 4 (a) Distribution on line of Al and O on the eutectic in the center of which contains a inclusion (SEM); (b) distribution on line of Mg, Mn and S on the eutectic in the center of which contains a inclusion (SEM); (c) distribution on line of Al after the eutectic removed (SEM); (d) growth of eutectic on MgS (TEM); (e) diffraction patterns, $B = [5\bar{1}0\bar{1}]_{\text{MgS}}$, $B_{\text{Fe}_3\text{C}} = [010]$; (f) growth of eutectic on CeO_2 (TEM); (g) diffraction patterns, $B_{\text{CeO}_2} = [01\bar{1}]$, $B_{\gamma\text{-Fe}} = [011]$, $B_{\text{Fe}_3\text{C}} = [361]$.

microcutting and a few of fatigue peeling under low impact, and drilling, peeling hole and microcutting under high impact.

It can be seen in Fig. 11c–e that the granular eutectic has following functions:(1) the granular eutectics effectively the intruding of abrasives into the wear surface because the eutectic has high microhardness (HV800-

1200), which makes the plough channel in length decrease. (2) the eutectic impedes microcutting of abrasives during microcutting, which makes the plough channel in depth.

Fig. 11f–h show the microstructures in the worn surface layer of ABGE composite. It can be seen that there are strain-induced martensite, dislocation and

TABLE IV Wear test results for some steels under different impact energy

Specimen*	0.5 J		1.0 J		1.5 J		2.0 J	
	Wear loss (mg)	ϵ	Wear loss (mg)	ϵ	Wear loss (mg)	ϵ	Wear loss (mg)	ϵ
Medium Mn steel with nodular carbide [6]	0.0436	0.72	0.1050	0.95	0.1176	0.99	0.1585	0.87
Austenite-bainite steel	0.0312	1.00	0.0994	1.00	0.1166	1.00	0.1379	1.00
Austenite-bainite nodular cast iron	0.0328	0.95	0.1169	0.85	0.1404	0.83	0.1723	0.80
High Cr cast iron	0.0249	1.25	0.0849	1.17	0.1355	0.86	0.1746	0.79
ABGE composite	0.0267	1.17	0.0793	1.25	0.1014	1.15	0.1253	1.10

*Austenite-bainite steel HRC: 47–50, Austenite-bainite nodular cast iron HRC: 43–45, High Cr cast iron HRC: 60–63.

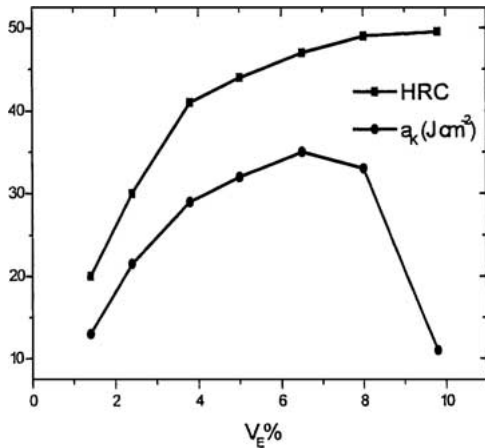


Figure 5 HRC and a_k of ABGE composite vs eutectic content (V_E).

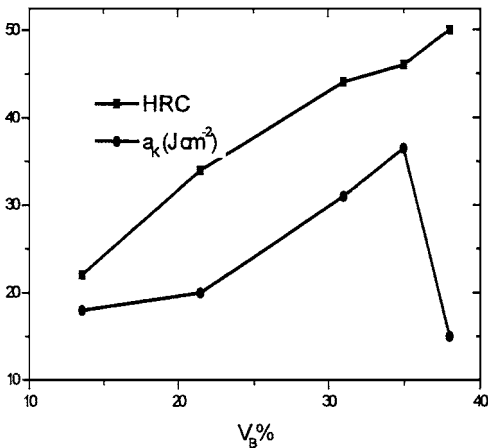


Figure 6 HRC and a_k of ABGE composite vs eutectic content (V_B).

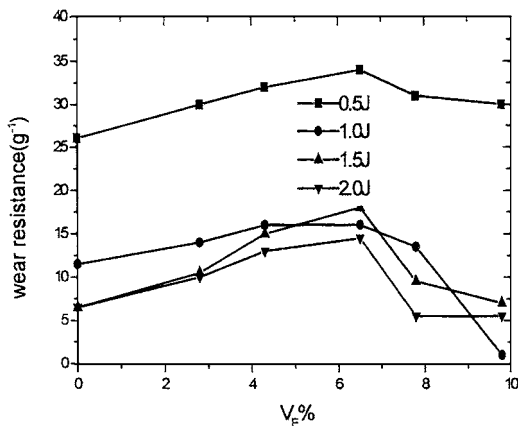


Figure 7 Effect of eutectic content on wear resistance of ABGE composite under different impact energy.

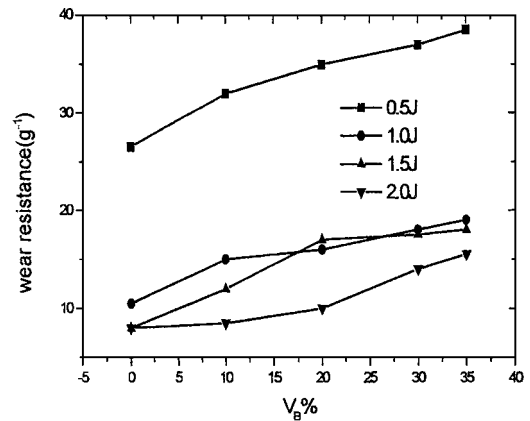


Figure 8 Effect of bainite content on wear resistance of ABGE composite under different impact energy.

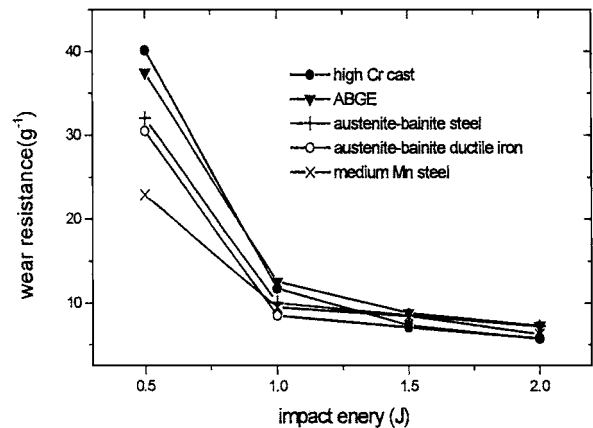


Figure 9 Contrast diagram of wear resistance of ABGE composite with existing wear-resistant materials.

deformed bainite in the worn surface layer, which makes the hardness in worn surface increase, as shown in Fig. 10. The bainite in the worn surface layer is deformed only, and it still consists of austenite film and ferrite, which has good ability to plastic deformation.

The deformed bainite can slacken expansion force of the phase transition when austenites between the bainites transform to strain induced martensite. At the same time, the deformed bainite in the worn surface layer can inhibit the initiation and spread of fatigue crack, improve the resistance to impact fatigue and decrease impact fatigue wear. Therefore, the worn surface of this composite has good hardness and toughness

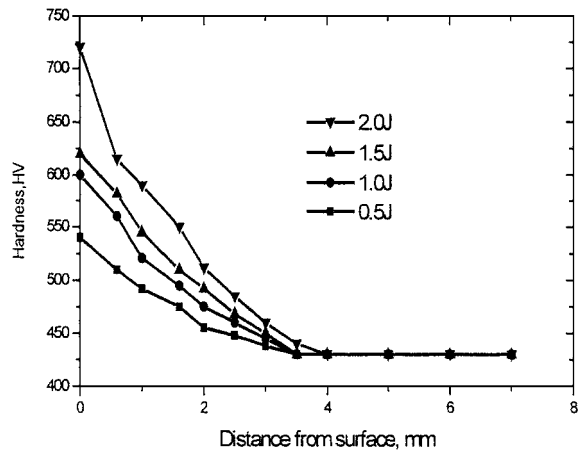


Figure 10 Hardness distribution of worn surface of ABGE composite under different impact energy.

because there are a large amount of strain induced martensite, dislocations and deformed bainites in the worn surface layer, which can make extruded lip bear more plastic deformation and not fail.

As described above, the ABGE composite possesses excellent wear resistance because the granular eutectics effectively the intrusion of abrasives into the wear surface and microcutting by abrasives on the worn surface,

and austenite-bainite matrix structure has high strain-hardening ability.

4. Conclusions

1. The ABGE composite can be obtained by alloying with manganese and silicon, modified by Al-Mg-Ce compound, air-hardening.

2. The granular eutectic is a pseudo-eutectic of austenite and $(Fe, Mn)_3C$, which is formed between austenite dendrites during solidification due to the segregation of C and Mn enhanced by modifying elements. The granulation of the eutectic can be explained by the heterogeneous nuclei of MgS and CeO_2 and by the influence of the modifying elements on the crystallization of the eutectic.

3. The granular eutectics effectively the intrusion of abrasives into wear surface and microcutting by abrasives on the worn surface. The worn surface of this composite has good hardness and toughness because there are a large amount of strain induced martensite, dislocation and deformed bainite in the worn surface layer, which can bear the abrasive impact and indentation.

4. The ABGE composite is a promising candidate material to resist abrasive wear under low and medium impact working condition.

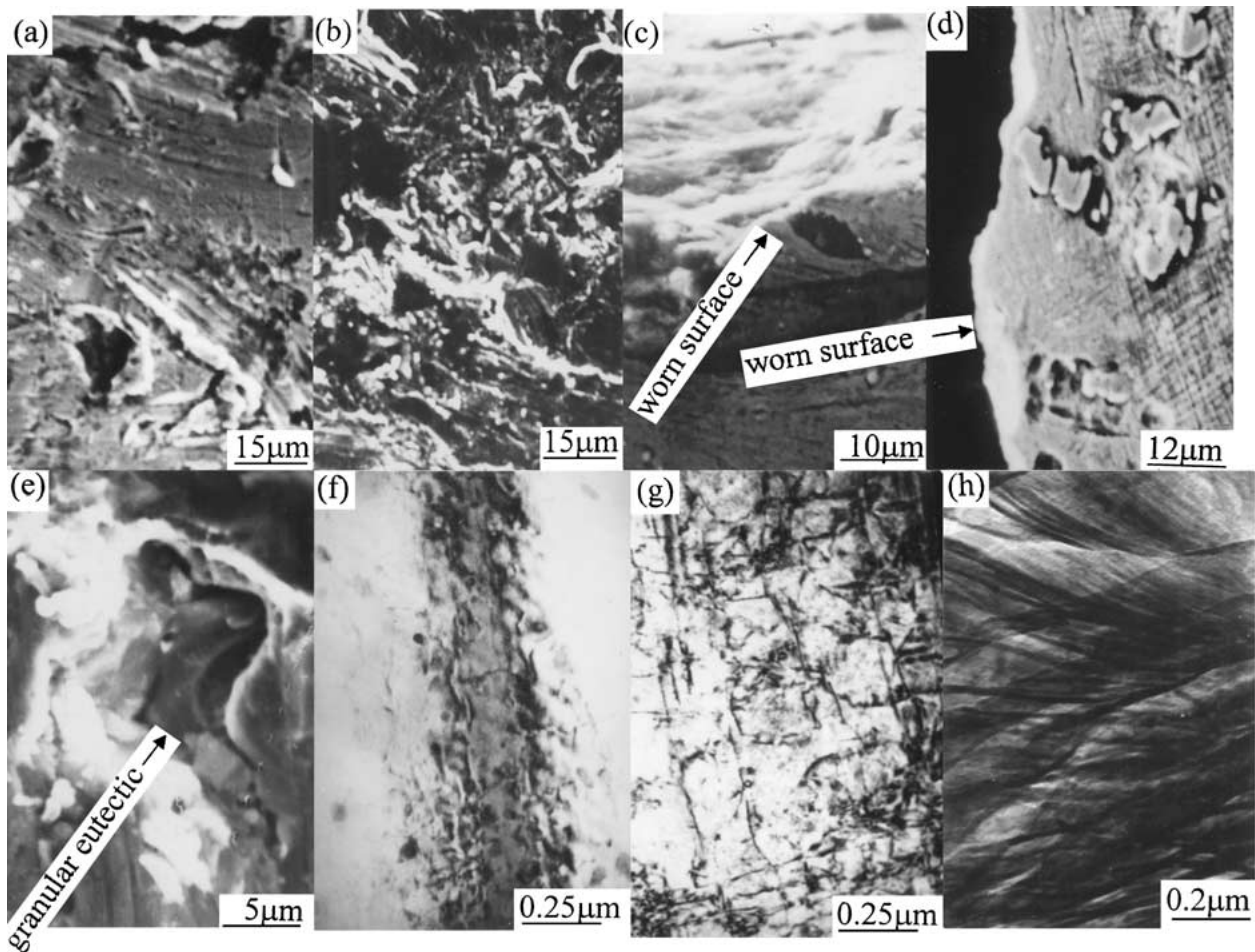


Figure 11 (a) Worn surface for ABGE composite under 0.5 J (SEM); (b) worn surface for ABGE composite under 2.0 J (SEM); (c) worn subsurface of ABGE composite with $V_E = 0.0\%$ (SEM); (d) worn subsurface of ABGE composite with $V_E = 6.5\%$ (SEM); (e) the eutectic on the worn surface (SEM); (f) strain induced martensite in the worn subsurface (TEM); (g) dislocation in the worn subsurface (TEM); (h) deformed bainite in the worn subsurface (TEM).

Acknowledgement

This work was supported by the National Science Foundation of China (No. 50001008).

References

1. H. M. WANG, H. S. SHAO and J. X. QU, *Chin. J. Mechanical Eng.* **4** (1991) 230 (in Chinese).
2. B. Q. WEI, J. LIANG and D. H. WU, *J. Mechan. Eng.* **27** (1991) 51 (in Chinese).
3. XU ZHENMING, JIANG QICHUAN and HE ZHENMING, *Tribology* **19** (1999) 39 (in Chinese).
4. HE ZHENMING, JIANG QICHUAN and FU SHAOBO, *Wear* **120** (1987) 305.
5. DER-HANG and GARETH THEOMAS, *Met. Trans.* **8A** (1977) 1661.
6. J. QICHUAN and H. ZHENMING, *J. Mater. Sci. Lett.* **9** (1990) 616.
7. XU ZHENMING, JIANG QICHUAN and HE ZHENMING, *Journal of Rare Earths* **6** (1998) 128.
8. B. L. BRAMFITT, *Met. Trans.* **1** (1970) 1987.
9. C. BODSWORTH and H. B. BALL, "Physical Chemistry of Iron and Manufacture," 2nd ed. (Longmans, London, 1972) p. 485.
10. XU ZHENMING, Dissertation of Harbin Institute of Technology (in Chinese) 1996, p. 65.
11. LIANG GONGYING and SHU ZHUNYI, *Cast Metals* **4** (1993) 4.

*Received 7 February 2000
and accepted 17 April 2001*